Dynamics of the Rotating Cantilever Beam

Aleksandar Nikolić[1*], Slaviša Šalinić[1]
[1]Faculty of Mechanical and Civil Engineering
University of Kragujevac, 36000 Kraljevo, Dositejeva 19 (Serbia)

This paper presents the dynamic analysis of a rotating cantilever beam with a tip mass by using the rigid segment method. The elastic beam is discretized into the number of rigid segments which are interconnected by elastic joint elements with three degrees of freedom. The dynamic analysis is performed by using absolute coordinates in the frame of Euler-Bernoulli beam theory. The critical angular velocity at which instability of the proposed solution occurs is determined.

Keywords: Rotating cantilever beam, rigid segment method, critical angular velocity

1. INTRODUCTION

Until now, the dynamic behavior of the flexible rotating beams has been investigated by many researches. The motive for this research lie in the fact that many engineering objects should be modelled as a rotating cantilever beam. Some of them are light robot arms, helicopter rotor blades, turbine blades, satellite linkages, etc. Modern industry has a need for machines of high-speed, increased accuracy and with the lowest possible weight. So, the rotational elements are lightweight and highly flexible. To ensure the accuracy of the motion of such elements, it is necessary to have an efficient control algorithm. Therefore, it is important to form a model of the flexible rotating beam that is simple and sufficiently accurate. The literature that deals with this problem is plenty (e.g. see [1-5]).

In this paper the rigid segment method will be used for the dynamic analysis of the flexible rotating cantilever beam with a tip mass. The basics about using this method in the free vibration analysis of the beams with variable axial parameters are described in [6] and [7] in detail. Here, this method will be adopted for the using in the analysis of the rotating flexible cantilever beam.

2. THE RIGID SEGMENT MODEL

Consider a hub beam system, shown in Fig 1. The hub is rigid and has the radius $\overline{OA} = r$. The flexible beam of a length L is rigidly connected to the hub at the point A. The beam material has the Young’s modulus E and the mass density ρ. Also, the beam cross section area is A, and the beam cross section moment of inertia is I_z. A tip mass m_T is fixed at the free end B of the beam. Let's introduce the two coordinate systems that are necessary for the rotation analysis of the system considered. The first one is the inertial fixed coordinate system $Oxyz$, and the second one is the reference frame $O\xi\eta\zeta$ whose axis ξ coincides with the direction of the undeformed beam. The angle θ defines the rotation of the reference coordinate system $O\xi\eta\zeta$ relative to the inertial coordinate system $Oxyz$.

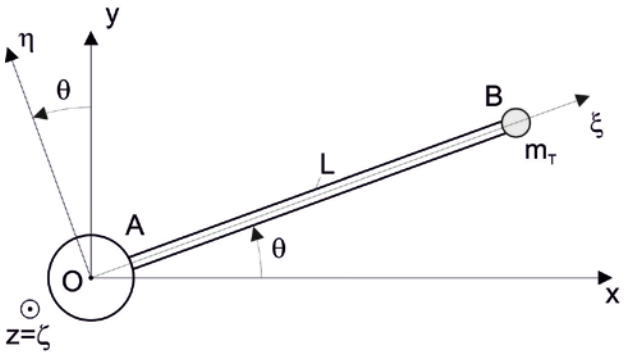

Figure 1: The rotating cantilever beam with a tip mass

Based on [5,6] the beam discretization is performed through two steps. At the first step, the beam is divided into n elastic segments which has the length L/n (see Fig 2(a)). After that, at the second step, all of the introduced elastic segments are replaced with two rigid segments of the length $L/(2n)$ which are mutually connected by the elastic joint elements JE_i $(i=1,\ldots,n)$ (see Fig 2(c)). The joint element JE_i allows three degrees of freedom, that are two relative translations in the axial and transverse direction, p_i and q_i, respectively, and one relative rotation r_i around the axis that is perpendicular to the motion plane. As mentioned above, the joint element JE_i is elastic, so the cylindrical and spiral springs are placed in the direction of the axial and rotational relative displacements, respectively (see Fig 2(d)). Based on [6], the stiffnesses of the introduced springs are:

$$c_{p_i} = n\frac{AE}{L},\ c_{q_i} = 12n^3\frac{EI_z}{L^3},\ c_{r_i} = n\frac{EI_z}{L^3}. \qquad (1)$$

Finally, the rigid segment model of the rotating flexible cantilever beam with the tip mass is formed as a system of $n+1$ rigid segments which are mutually connected by n elastic joint elements JE_i (see Fig 2(b)).

For the purpose of further analysis, let’s define the physical parameters of the introduced rigid segments. The length, mass and rotational inertia of the rigid segments should be defined as:

*Corresponding author: Faculty of Mechanical and Civil Engineering, University of Kragujevac, 36000 Kraljevo, Dositejeva 19 (Serbia), nikolic.a@mfkv.kg.ac.rs

$$l_i = \begin{cases} R + L/(2n), & i = 0, \\ L/n, & 0 < i < n, \\ L/(2n), & i = n, \end{cases} \tag{2}$$

$$m_i = \begin{cases} m_h + \rho AL/(2n), & i = 0, \\ \rho AL/n, & 0 < i < n, \\ \rho AL/(2n) + m_T, & i = n, \end{cases} \tag{3}$$

$$J_{C_i\zeta} = \begin{cases} J_h + m_h \overline{O_0C_0}^2 + \frac{1}{12}\rho A\left(\frac{L}{2n}\right)^3 \\ +\rho A \frac{L}{2n}\left(\overline{O_0C_0} - \frac{L}{4n}\right)^2, & i = 0, \\ \frac{1}{12} m_i l_i^2, & 0 < i < n, \\ \frac{1}{12}\rho A l_n^3 + \rho A l_n \left(\overline{O_nC_n} - \frac{L}{4n}\right)^2 \\ +m_T\left(\frac{L}{2n} - \overline{O_nC_n}\right)^2, & i = n, \end{cases} \tag{4}$$

respectively, where

$$\overline{O_iC_i} = \begin{cases} \frac{\rho AL\left(R + L/(4n)\right)}{2n \cdot m_h + \rho AL}, & i = 0, \\ l_i/2, & 0 < i < n, \\ \frac{L\left(\rho AL + 4n \cdot m_T\right)}{4n\left(\rho AL + 2n \cdot m_T\right)}, & i = n, \end{cases} \tag{5}$$

is the distance of the mass center from the left side of the rigid segment (Vi).

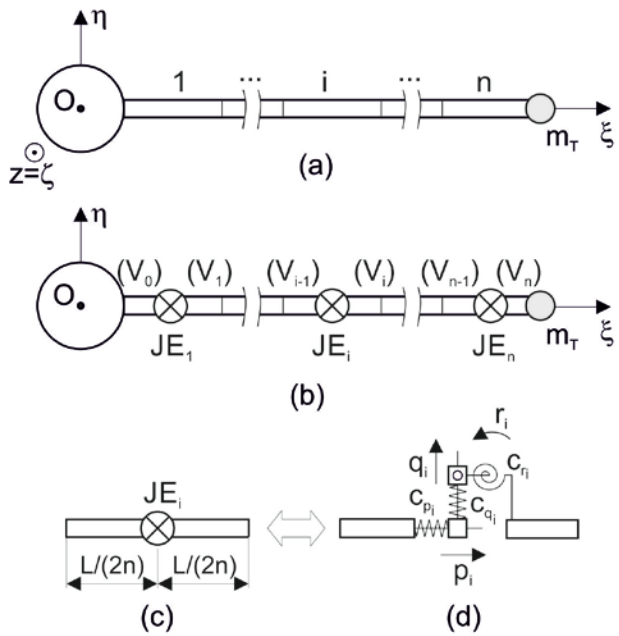

Figure 2: Discretization of the elastic beam into rigid segments and elastic joint elements

3. DIFFERENTIAL EQUATIONS OF MOTION

During the rotation, the flexible beam deforms. Therefore, the position of the rigid segment (V_i) relative to the coordinate system Oξηζ should be defined with axial and transversal coordinates of the rigid segment mass center, ξ_i and η_i, respectively, and with rotation angle φ_i of the rigid segment relative to the undeformed state of the beam.

The axial coordinate ξ_i can be defined as:

$$\xi_i = \xi_i(0) + \tilde{\xi}_i, \tag{6}$$

where

$$\xi_i(0) = \begin{cases} \overline{O_0C_0}, & i = 0, \\ \sum_{k=0}^{i-1} l_k + \overline{O_iC_i}, & i > 0, \end{cases} \tag{7}$$

is the value of the axial coordinate in the undeformed state of the beam, and $\tilde{\xi}_i$ represents the value of the axial deformation relative to the undeformed state of the beam. In the undeformed state, the values of the transversal coordinate η_i and rotation angle φ_i has zero values (see Fig 3).

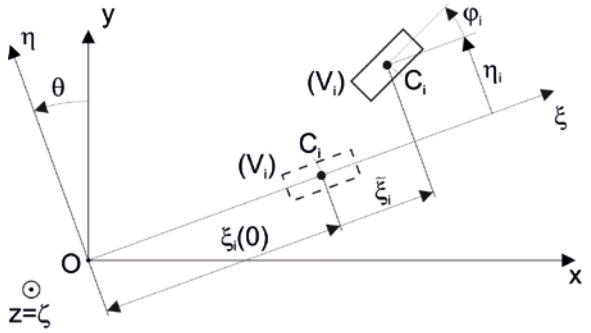

Figure 3: The motion of the rigid segment (V_i) during rotation

The kinetic energy of the rigid segment model reads:

$$T = \frac{1}{2}\sum_{i=0}^{n}\left(m_i v_i^2 + J_{C_i\zeta}\omega_i^2\right), \tag{8}$$

where v_i and ω_i are the velocity of the mass center and the angular velocity of the rigid segment (V_i), respectively. By using the above defined coordinates, the velocity v_i reads:

$$v_i^2 = \dot{x}_i^2 + \dot{y}_i^2, \tag{9}$$

where x_i and y_i are the coordinates of the mass center of the rigid segments (V_i) relative to the inertial coordinate system *Oxyz* are given as:

$$x_i = \xi_i \cos\theta - \eta_i \sin\theta, \tag{10}$$

$$y_i = \xi_i \sin\theta + \eta_i \cos\theta. \tag{11}$$

Taking into account the expression (6), the time derivatives of the previously defined coordinates read:

$$\dot{x}_i = \dot{\tilde{\xi}}_i \cos\theta - \left(\xi_i(0) + \tilde{\xi}_i\right)\dot{\theta}\sin\theta - \dot{\eta}_i \sin\theta - \eta_i\dot{\theta}\cos\theta, \tag{12}$$

$$\dot{y}_i = \dot{\tilde{\xi}}_i \sin\theta + \left(\xi_i(0) + \tilde{\xi}_i\right)\dot{\theta}\cos\theta + \dot{\eta}_i \cos\theta - \eta_i\dot{\theta}\sin\theta. \tag{13}$$

Now, by using the expressions (6), (9), (12), and (13), the velocity of the rigid segment (V_i) mass center takes the following form:

$$v_i^2 = \dot{\tilde{\xi}}_i^2 + \dot{\eta}_i^2 + 2\left(\left(\xi_i(0)+\tilde{\xi}_i\right)\dot{\eta}_i - \eta_i\dot{\tilde{\xi}}_i\right)\dot{\theta} + \left(\left(\xi_i(0)+\tilde{\xi}_i\right)^2 + \eta_i^2\right)\dot{\theta}^2, \quad (14)$$

The angular velocity of the rigid segment (V_i) is given as:

$$\omega_i = \dot{\theta} + \dot{\varphi}_i. \quad (15)$$

By inserting the expressions (14) and (15) into the expression (8), the kinetic energy of the rigid segment model becomes:

$$T = \frac{1}{2}\sum_{i=0}^{n}\left(m_i\left(\dot{\tilde{\xi}}_i^2 + \dot{\eta}_i^2 + 2\left(\left(\xi_i(0)+\tilde{\xi}_i\right)\dot{\eta}_i - \eta_i\dot{\tilde{\xi}}_i\right)\dot{\theta} + \left(\left(\xi_i(0)+\tilde{\xi}_i\right)^2 + \eta_i^2\right)\dot{\theta}^2\right) + J_{C_i\zeta}\left(\dot{\theta}+\dot{\varphi}_i\right)^2\right), \quad (16)$$

The potential energy of the rigid segment model reads:

$$\Pi = \frac{1}{2}\sum_{i=1}^{n}\left(c_{p_i}p_i^2 + c_{q_i}q_i^2 + c_{r_i}r_i^2\right), \quad (17)$$

where p_i, q_i, and r_i represent the relative displacements in the elastic joint element JE_i (see Fig 2(d)).

By using the small deformation assumption, the relative displacements p_i, q_i, and r_i should be obtained by using the rigid segments coordinates in the reference coordinate system Oξηζ as:

$$p_i = -\tilde{\xi}_{i-1} + \tilde{\xi}_i, \quad (18)$$

$$q_i = -\eta_{i-1} + \eta_i - \frac{l_{i-1}}{2}\varphi_{i-1} - \frac{l_i}{2}\varphi_i, \quad (19)$$

$$r_i = -\varphi_{i-1} + \varphi_i. \quad (20)$$

Inserting the expressions (18)-(20) into the expression (17), the potential energy of the rigid segment model takes the following form:

$$\Pi = \frac{1}{2}\sum_{i=1}^{n}\left(c_{p_i}\left(-\tilde{\xi}_{i-1}+\tilde{\xi}_i\right)^2 + c_{q_i}\left(-\eta_{i-1}+\eta_i - \frac{l_{i-1}}{2}\varphi_{i-1} - \frac{l_i}{2}\varphi_i\right)^2 + c_{r_i}\left(-\varphi_{i-1}+\varphi_i\right)^2\right). \quad (21)$$

Now, the differential equations of motion of the considered rigid segment model may be obtained by using the Lagrange equations of the second kind [8]:

$$\frac{d}{dt}\frac{\partial T}{\partial \dot{\tilde{\xi}}_i} - \frac{\partial T}{\partial \tilde{\xi}_i} = -\frac{\partial \Pi}{\partial \tilde{\xi}_i} + Q_{\tilde{\xi}_i}, \quad (22)$$

$$\frac{d}{dt}\frac{\partial T}{\partial \dot{\eta}_i} - \frac{\partial T}{\partial \eta_i} = -\frac{\partial \Pi}{\partial \eta_i} + Q_{\eta_i}, \quad (23)$$

$$\frac{d}{dt}\frac{\partial T}{\partial \dot{\varphi}_i} - \frac{\partial T}{\partial \varphi_i} = -\frac{\partial \Pi}{\partial \varphi_i} + Q_{\varphi_i}, \quad (24)$$

where $i=1,\ldots,n$,and $Q_{\tilde{\xi}_i} = Q_{\eta_i} = Q_{\varphi_i} = 0$.

By using the expressions for the kinetic and potential energies, (16) and (17), the differential equations of motion (22)-(24) become:

$$m_i\ddot{\tilde{\xi}}_i - 2m_i\dot{\theta}\dot{\eta}_i - c_{p_i}\tilde{\xi}_{i-1} + \left(c_{p_i} + c_{p_{i+1}} - m_i\dot{\theta}^2\right)\tilde{\xi}_i - c_{p_{i+1}}\tilde{\xi}_{i+1} = m_i\xi_i(0)\dot{\theta}^2 + m_i\eta_i\ddot{\theta}, \quad (25)$$

$$m_i\ddot{\eta}_i - 2m_i\dot{\theta}\dot{\tilde{\xi}}_i - c_{q_i}\eta_{i-1} - \frac{l_{i-1}}{2}c_{q_i}\varphi_{i-1} + \left(c_{q_i} + c_{q_{i+1}} - m_i\dot{\theta}^2\right)\eta_i - \frac{l_i}{2}\left(c_{q_i} - c_{q_{i+1}}\right)\varphi_i - c_{q_{i+1}}\eta_{i+1} + \frac{l_{i+1}}{2}c_{q_{i+1}}\varphi_{i+1} = -m_i\left(\xi_i(0)+\tilde{\xi}_i\right)\ddot{\theta}, \quad (26)$$

$$J_{C_i\zeta}\ddot{\varphi}_i + \frac{l_i}{2}c_{q_i}\eta_{i-1} + \left(-c_{r_i} + \frac{l_i l_{i-1}}{4}c_{q_i}\right)\varphi_{i-1} + \frac{l_i}{2}\left(-c_{q_i} + c_{q_{i+1}}\right)\eta_i + \left(c_{r_i} + c_{r_{i+1}} + \frac{l_i^2}{4}\left(c_{q_i} + c_{q_{i+1}}\right)\right)\varphi_i - \frac{l_i}{2}c_{q_{i+1}}\eta_{i+1} + \left(\frac{l_i l_{i+1}}{4}c_{q_{i+1}} - c_{r_{i+1}}\right)\varphi_{i+1} = -J_{C_i\zeta}\ddot{\theta}, \quad (27)$$

where $i=1,\ldots,n$, $\tilde{\xi}_0 = \tilde{\xi}_{n+1} = 0$, $\eta_0 = \eta_{n+1} = 0$, and $\varphi_0 = \varphi_{n+1} = 0$.

After summing, the above defined differential equations of motion (25)-(27) should be written in a matrix form as:

$$\mathbf{M}_v\ddot{\mathbf{v}} + \left(\mathbf{K} - \dot{\theta}^2\mathbf{M}_m\right)\mathbf{v} - 2\mathbf{M}_{mv}\dot{\mathbf{v}}\dot{\theta} = \mathbf{M}_{\theta v}\ddot{\theta} + \mathbf{M}_{m\xi}\dot{\theta}^2, \quad (28)$$

where

$$\mathbf{v} = \left[\tilde{\xi}_1, \eta_1, \varphi_1, \ldots, \tilde{\xi}_i, \eta_i, \varphi_i, \ldots, \tilde{\xi}_n, \eta_n, \varphi_n\right]^T, \quad (29)$$

$$\mathbf{M}_v = diag\left(\mathbf{M}_{v_1}, \ldots, \mathbf{M}_{v_i}, \ldots, \mathbf{M}_{v_n}\right) \in R^{3n\times 3n}, \quad (30)$$

$$\mathbf{M}_{v_i} = diag\left(m_i, m_i, J_{C_i\zeta}\right) \in R^{3\times 3}, \quad (31)$$

$$\mathbf{K} = \begin{bmatrix} \mathbf{K}_{22}^{(1)} + \mathbf{K}_{11}^{(2)} & \mathbf{K}_{12}^{(2)} & \mathbf{0} & \mathbf{0} \\ \mathbf{K}_{21}^{(2)} & \mathbf{K}_{22}^{(2)} + \mathbf{K}_{11}^{(3)} & \mathbf{K}_{12}^{(3)} & \mathbf{0} \\ \mathbf{0} & \vdots & \ddots & \vdots \\ \vdots & \mathbf{0} & \mathbf{K}_{21}^{(i-1)} & \mathbf{K}_{22}^{(i-1)} + \mathbf{K}_{11}^{(i)} \\ \vdots & \vdots & \mathbf{0} & \vdots \\ \vdots & \vdots & \vdots & \mathbf{0} \\ \mathbf{0} & \mathbf{0} & \mathbf{0} & \mathbf{0} \end{bmatrix}$$

$$\begin{bmatrix} \mathbf{0} & \mathbf{0} & \mathbf{0} \\ \vdots & \vdots & \vdots \\ \mathbf{0} & \vdots & \vdots \\ \mathbf{K}_{12}^{(i)} & \mathbf{0} & \vdots \\ \ddots & \vdots & \mathbf{0} \\ \mathbf{K}_{21}^{(n-1)} & \mathbf{K}_{22}^{(n-1)} + \mathbf{K}_{11}^{(n)} & \mathbf{K}_{12}^{(n)} \\ \mathbf{0} & \mathbf{K}_{21}^{(n)} & \mathbf{K}_{22}^{(n)} \end{bmatrix} \in R^{3n\times 3n}, \quad (32)$$

$$\mathbf{K}_{11}^{(i)}=\begin{bmatrix} c_{p_i} & 0 & 0 \\ 0 & c_{q_i} & \frac{l_{i-1}}{2}c_{q_i} \\ 0 & \frac{l_{i-1}}{2}c_{q_i} & c_{r_i}+\frac{l_{i-1}^2}{4}c_{q_i} \end{bmatrix}, \quad (33)$$

$$\mathbf{K}_{12}^{(i)}=\begin{bmatrix} -c_{p_i} & 0 & 0 \\ 0 & -c_{q_i} & \frac{l_i}{2}c_{q_i} \\ 0 & -\frac{l_{i-1}}{2}c_{q_i} & \frac{l_{i-1}l_i}{4}c_{q_i}-c_{r_i} \end{bmatrix}, \quad (34)$$

$$\mathbf{K}_{12}^{(i)}=\left(\mathbf{K}_{21}^{(i)}\right)^T, \quad (35)$$

$$\mathbf{K}_{22}^{(i)}=\begin{bmatrix} c_{p_i} & 0 & 0 \\ 0 & c_{q_i} & -\frac{l_i}{2}c_{q_i} \\ 0 & -\frac{l_i}{2}c_{q_i} & \frac{l_i^2}{4}c_{q_i}+c_{r_i} \end{bmatrix}, \quad (36)$$

$$\mathbf{M}_m=diag\left(\mathbf{M}_{m_1},\ldots,\mathbf{M}_{m_i},\ldots,\mathbf{M}_{m_n}\right)\in R^{3n\times 3n}, \quad (37)$$

$$\mathbf{M}_{m_i}=diag\left(m_i,m_i,0\right), \quad (38)$$

$$\mathbf{M}_{mv}=diag\left(\mathbf{M}_{mv_1},\ldots,\mathbf{M}_{mv_i},\ldots,\mathbf{M}_{mv_n}\right)\in R^{3n\times 3n}, \quad (39)$$

$$\mathbf{M}_{mv_i}=\begin{bmatrix} 0 & m_i & 0 \\ m_i & 0 & 0 \\ 0 & 0 & 0 \end{bmatrix}, \quad (40)$$

$$\mathbf{M}_{\theta v}=\left[\mathbf{M}_{\theta v_1},\ldots,\mathbf{M}_{\theta v_i},\ldots,\mathbf{M}_{\theta v_n}\right]^T\in R^{3n\times 1}, \quad (41)$$

$$\mathbf{M}_{\theta v_i}=\left[m_i\eta_i,-m_i\left(\xi_i(0)+\tilde{\xi}_i\right),-J_{C_i\zeta}\right]^T, \quad (42)$$

$$\mathbf{M}_{m\xi}=\left[\mathbf{M}_{m\xi_1},\ldots,\mathbf{M}_{m\xi_i},\ldots,\mathbf{M}_{m\xi_n}\right]^T\in R^{3n\times 1}, \quad (43)$$

$$\mathbf{M}_{m\xi_i}=\left[m_i\xi_i(0),0,0\right]^T. \quad (44)$$

4. NUMERICAL SIMULATIONS AND RESULTS

The physical parameters of the beam which will be used here are follows:

- Length L=8 [m],
- Mass density ρ =2.7667·10^3 [kg/m^3],
- Cross-section area A=7.2968·10^{-5} [m^2],
- Young’s modulus E=6.8952·10^{10} [N/m^2],
- Cross-section moment of inertia I_z =8.2189·10^{-9} [m^4],
- Hub moment of inertia J_h =200 [kg·m^2],
- Hub radius r =0.5 [m],
- Tip mass m_T =(0.1-0.5) [kg].

It is also assumed that the angular velocity of the considered hub beam system is defined as a time function of the form:

$$\dot{\theta}=\begin{cases} \frac{w_f}{t_f}t-\frac{w_f}{2\pi}\sin\left(\frac{2\pi}{t_f}t\right), & 0\le t\le t_f, \\ w_f, & t>t_f, \end{cases} \quad (45)$$

where w_f represents the stationary angular velocity of the hub beam system that will be achieved after time period t_f.

The Runge-Kutta method of the fourth order is used for the numerical integration of the differential equations of motion (28). Also, the elastic beam is discretized into 20 elastic segments, that is n=20.

Figure 4 shows the response of the beam tip along the transverse and the axial direction during the rotation. It is assumed that there is no tip mass, eg m_T =0, t_f =15 [s], and that the steady state angular velocity w_f has the values 1, 2 and 4 [rad/s]. In the case w_f =2 [rad/s] our results for the transversal displacements shown in Fig 4(a) are the same as those ones from [4] obtained by the using zero order model (linear model).

Is is obvious that by increasing w_f from 1 [rad/s] to 2[rad/s], the maximum deflection in the both transverse and axial beam direction increases, too. For the w_f =4 [rad/s], the results obtained by using the presented approach are divergent. The identically divergent result is obtained in [4] when the zero order model was used.

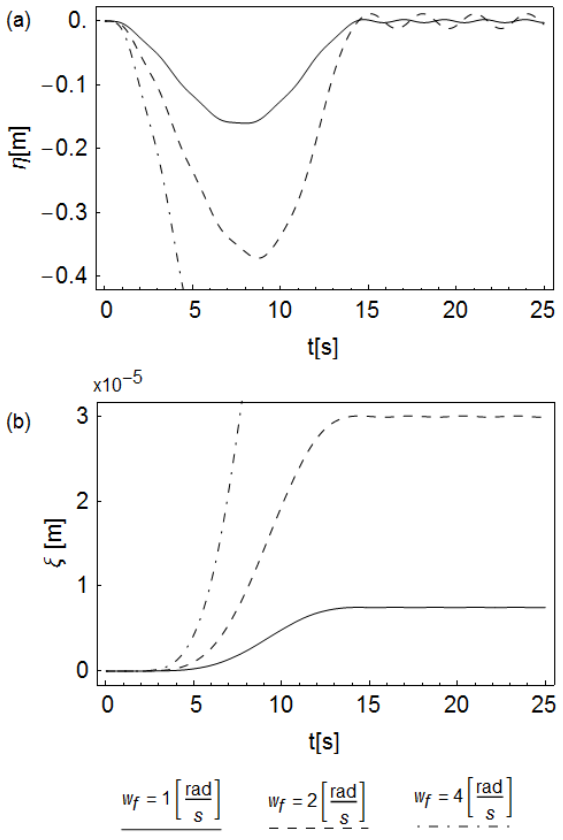

Figure 4: The beam tip response under the rotation:

(a) *transversal direction, (b) axial direction.*

The reason for the divergence of the results can be found by analyzing the differential equations of motion (28). Namely, the generalized stiffness matrix is defined by the matrix $\mathbf{K}-\dot{\theta}^2\mathbf{M}_m$. As the angular velocity of the

hub-beam system $\dot{\theta}$ increases, the same elements of the generalized stiffness matrix decrease. When the angular velocity $\dot{\theta}$ reached some critical value, the generalized stiffness matrix is singular, and the solutions become divergent. So, the critical value of the angular velocity at which the presented rigid segment method failed to describe the dynamics of the rotating cantilever beam should be obtained by solving the following equation:

$$\left|\mathbf{K}-\dot{\theta}_{cr}^2\mathbf{M}_m\right|=0. \tag{33}$$

As the matrix $\mathbf{M}_m$ depends on the masses of rigid segments (see (37) and (38)), the value of the critical angular velocity $\dot{\theta}_{cr}$ decreases with the increasing of the tip mass m_T. The above statement is proved in Table 1. In the case when m_T=0, the critical angular velocity is $\dot{\theta}_{cr}=2.91[\text{rad/s}]$. But, for m_T=1 [kg], the value of the critical angular velocity significantly decreases to $\dot{\theta}_{cr}=1.55[\text{rad/s}]$. Better insight into this dependance should be obtained by analyzing Figure 5.

Table 1: The values of the critical angular velocity corresponding to the different tip mass values

m_T [kg]	0	0.1	0.3	0.5	0.7	0.9	1
$\dot{\theta}_{cr}$ [rad/s]	2.91	2.61	2.20	1.94	1.75	1.61	1.55

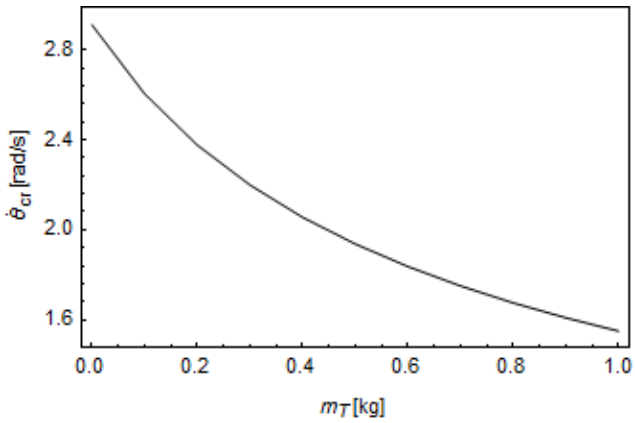

Figure 5: The impact of the tip mass to the critical angular velocity

Now, by analyzing the Table 1, we can determine the critical angular velocity at which divergence of the results occurs. Figure 6 shows the response of the beam tip in the transverse and axial direction during the rotation for m_T =0.1 [kg] and t_f =30 [s]. The value of the critical angular velocity for the given parameters is $\dot{\theta}_{cr}=2.61[\text{rad/s}]$. When the steady state angular velocity is less than critical value w_f=2 [rad/s], the obtained results are correct. However, when the steady state angular velocity exceeds the critical value, eg when w_f=2.7 [rad/s], the obtained results become divergent. The situation is similar when the tip mass increases to m_T =0.5 [kg]. In this case, the critical angular velocity decreases to $\dot{\theta}_{cr}=1.94[\text{rad/s}]$ (see Table 1).

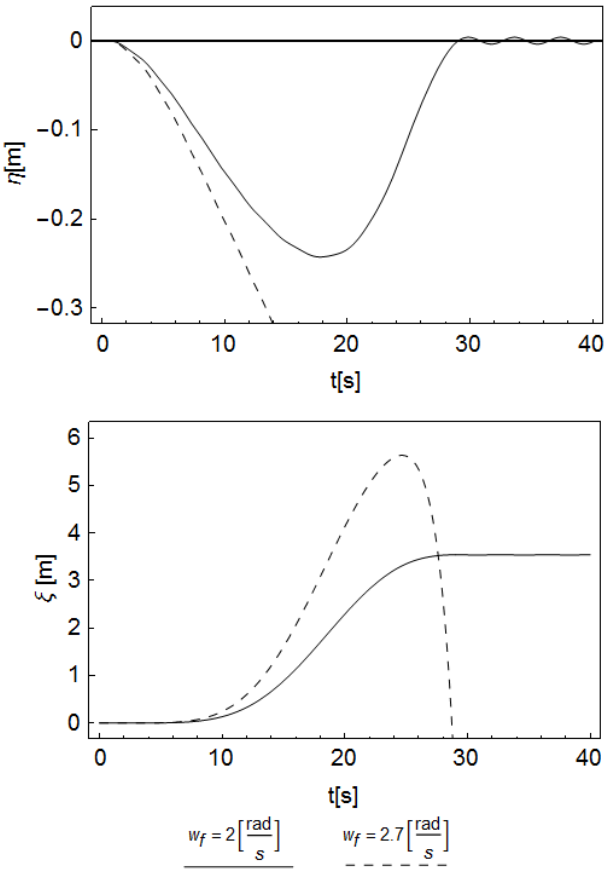

Figure 6: The beam tip response under the rotation at m_T=0.1 [kg]

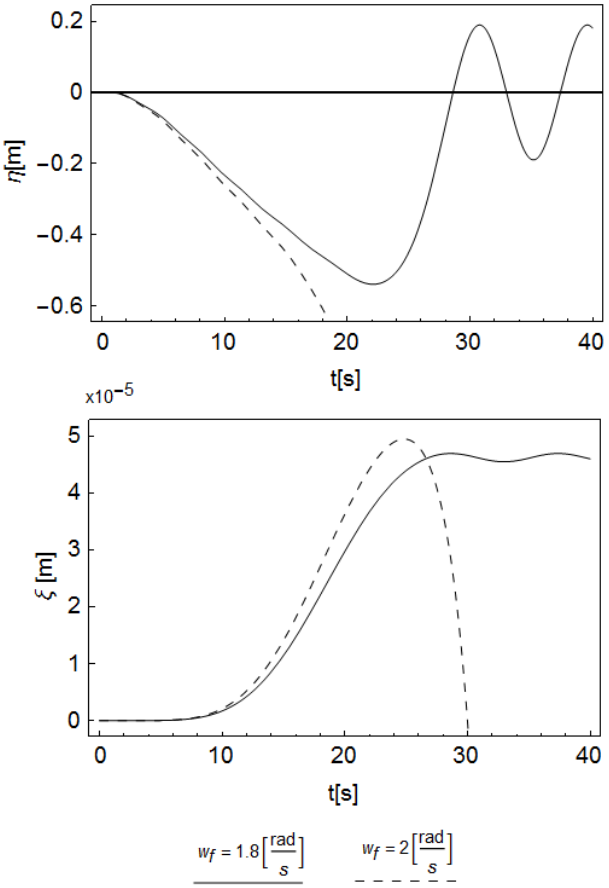

Figure 7: The beam tip response under the rotation at m_T=0.5 [kg]

When the steady state angular velocity is less than critical, w_f =1.8 [rad/s], the obtained results are correct. As in the previous case, when the steady state angular velocity exceeds the critical value, w_f =2 [rad/s], the results become divergent.

It is important to note that in both described cases (for m_T =0.1 [kg] and for m_T =0.5 [kg]) the obtained results for the transversal displacement $\eta(t)$ agrees very well with the results given in [1] obtained by using the traditional linear approximated model (TLAM). The values of the axial tip displacement $\xi(t)$ are not presented in [1].

5. CONCLUSION

In this paper the dynamic analysis of the flexible rotating cantilever beam by using the rigid segment method has been performed. The rigid segment model considers the bending as well as the axial deformation of the beam during rotation. The obtained differential equations of motion in a matrix form (28) allow the efficient dynamic analysis of the considered rotating beam. Because the small deformation assumption has been used the considered method is linear.

As observed in [5], the use of the linear model leads to the conditionally stable results. Namely, if the angular velocity of the hub reaches the critical value of the angular velocity, the generalized stiffness matrix becomes singular and the results are divergent. So, before the proposed rigid segment method being used, it is necessary to determine the value of the critical angular velocity by using the expression (33). The precision of the presented method is demonstrated by numerical examples in which the good agreement with the results from [1] and [4] has been achieved.

In the further research, the presented method can be improved by taking into account the large deformation of the considered beam during the rotation. As a result of this assumption, the generalized stiffness matrix would be non-linear. It is expected that by using the above assumption the critical angular velocity of the rotating beam will be increased.

ACKNOWLEDGEMENTS

This research was supported under grants no. ON174016 and no. TR35006 by the Ministry of Education, Science and Technological Development of the Republic of Serbia. This support is gratefully acknowledged.

REFERENCES

S. Bai, P. Ben-Tzvi, Q. Zhou, and X. Huang, “Dynamic modeling of a rotating beam having a tip mass”, Robotic and Sensors Environments- International Workshop (IEEE), ROSE, October 2008 ,pp. 52-57, (2008)

[1] Y. Wang, and R. L. Huston, "A lumped parameter method in the nonlinear analysis of flexible multibody systems", Comput. Struct., Vol. 50(3), pp 421-432, (1994)

[2] D.J. Zhang, R. L. Huston, "On dynamic stiffening of flexible bodies having high angular velocity", Journal of Structural Mechanics, Vol. 24(3), pp 313-329, (1996)

[3] C. Li, X. Meng, and Z. Liu, "Dynamic modeling and simulation for the rigid flexible coupling system with a non-tip payload in non-inertial coordinate system", J. Vib. Control, Vol. 22(4), pp.1076-1094, (2016)

[4] D. Garcia-Vallejo, H. Sugiyama, A. A. Shabana, “Finite element analysis of the geometric stiffening effect. Part 1: a correction in the floating frame of reference formulation”, P I Mech Eng K-J Mul, Vol. 219(2), pp. 187-202, (2005)

[5] A. Nikolić, S. Šalinić, “A rigid multibody method for free vibration analysis of beams with variable axial parameters”, J. Vib. Control, Vol. 23(1), pp. 131 – 146, (2017)

[6] A. Nikolić, “Free vibration analysis of a non-uniform axially functionally graded cantilever beam with a tip body”, Arch. Appl. Mech., doi:10.1007/s00419-017-1243-z, (2017)

[7] A. I. Lurie, “Analytical Mechanics”, Springer-Verlag, New York, 2002.